Use of NOAA AVHR Digital Satellite Data for Precipitation and Forest Fire Assessment

by

Arnold M. Hougham

SRC Technical Report No. 198
August, 1987

SRC
Saskatchewan Research Council

Energy, Mines and Resources Canada

88-02196/

USE OF NOAA AVHRR DIGITAL SATELLITE DATA FOR PRECIPITATION AND FOREST FIRE ASSESSMENT

by

Arnold M. Hougham

SRC Technical Report No. 198

SRC Publication No. E-905-19-B-87
August, 1987

SUMMARY

Two resource problems, the impact of drought in semi-arid regions, and the detection of forest fires, can by solved by utilizing NOAA satellite data.

The study has concluded that:

a) The enhanced satellite data strongly indicate vegetation vigour, as controlled by precipitation during the growing season, over the whole of the agricultural region at one time.

b) The satellite system is capable of detecting fires as small as 0.09 hectares four times per day, including at night.

The study recommends:

a) That NOAA AVHRR data be obtained, during the period July 15 to July 31, on an annual basis. Data analysis would enable the monitoring of vegetation vigour over the whole of southern Saskatchewan to determine areas affected by drought.

b) That fire detection using the NOAA AVHRR system be implemented as a complement to current methods.

TABLE OF CONTENTS

Page

SUMMARY iii

PART 1: INTRODUCTION 1

PART 2: CHEMICAL IMPACTS DETECTION IN SOUTHERN SASKATCHEWAN USING NOAA AVHRR DATA 3
- INTRODUCTION 3
- METHODOLOGY 4
- DISCUSSION 6
- CONCLUSION 7

PART 3: FOREST FIRE DETECTION IN NORTHERN SASKATCHEWAN USING NOAA AVHRR CHANNEL 3 DATA 11
- INTRODUCTION 11
- METHODOLOGY 12
- DISCUSSION 15
- CONCLUSION 16

Page

PART 4: CONCLUSIONS AND RECOMMENDATIONS 19
- CONCLUSIONS 19
- RECOMMENDATIONS 19

REFERENCES 21
- ACKNOWLEDGEMENTS 22

APPENDIX 23
- METHODOLOGY 23
- ANNEX A 25
- ANNEX B 26
- ANNEX C 27

LIST OF FIGURES

Page

Figure 1. Study area showing crop district boundaries and precipitation stations 4

Figure 2. Average monthy precipitation to July in each of the four test years 5

Figure 3. The normalized difference vegetation index (NDVI) as a function of monthly rainfall for each test period 7

Figure 4. NDVI as a function of monthly rainfall for all four years 8

Figure 5. NDVI differences (from 1983 data) plotted against precipitation differences for the same years 8

Page

Figure 6. Climates of the continents according to Koppen Classification. Areas with negative soil moisture budget have a "B" designation (from Briggs and Smithson, 1985 9

Figure 7. Planck radiances for temperatures from 200 K to 500 K. For a given increase in temperature, the increase in area under the channel segments of the curves is much greater than under the channel 4 segments 12

Figure 8. An example of forest fire detection from a specific satellite image 14

LIST OF TABLES

Page

Table 1. AVHRR Channelization 1

Table 2. NDVI and Precipitation Data by Area 6

Table 3. Precipitation and Correlation Statistics for Study Area 6

Page

Table 4. Forest Fire Locations and Sizes 13

Table 5. Comparison of Known Fires with Detected Fires 16

PART 1:
INTRODUCTION

In 1970, the U.S. National Oceanic and Atmospheric Administration launched the first of many polar orbiting "NOAA" satellites designed specifically for weather analysis and forecasting. Almost immediately, environmental scientists began to investigate the application of imagery from the sensors on board these satellites for other purposes. The Advanced Very High Resolution Radiometer (AVHRR) sensor provides imagery which has characteristics uniquely suited to environmental analysis over large areas. Nominal resolution at nadir is 1.1 km, and the system provides subcontinental image swaths twice daily. With two operational systems at this writing, global coverage is provided four times per day. The characteristics of the NOAA AVHRR system therefore provide appropriate data for environmental problems which require a "synoptic" view of large areas on a frequent basis.

Coupled with the system characteristics outlined above are the spectral characteristics for the AVHRR sensor itself. These spectral characteristics for the current NOAA AVHRR sensors are given in Table 1.

TABLE 1
AVHRR CHANNELIZATION

channel	spectral range (micrometres)
1.	0.58 - 0.68
2.	0.725 - 1.10
3.	3.55 - 3.93
4.	10.3 - 11.3
5.	11.5 - 12.5

from: Allison and Schnapf (1983)

Channels 1 and 2 are sensitive to vegetation characteristics; channel 1 responds to leaf chlorophyll content, and channel 2 responds to changes in leaf structure. Channel 3, commonly referred to as the "water absorption band", used primarily for assessing water vapour content of the atmosphere, responds to very hot sources. The characteristics of the NOAA AVHRR system make it a very useful data source for a variety of environmental problems. This Report examines the utility of these data for two applications of importance to Saskatchewan.

The vigour of Saskatchewan's agricultural zone vegetation is closely tied to the available moisture, the primary input being precipitation during the growing season. Special digital enhancement techniques have been developed using multispectral data in the visible and near infrared portions of the spectrum which, it has been suggested, reflect the vigour of the vegetation canopy. Thus, Part 2 of this Report examines the relationship between growing season precipitation and images produced using the above mentioned enhancement techniques. A methodology is outlined (Appendix) which allows the production of a digital product which exhibits vegetation vigour at a point in time over the whole of southern Saskatchewan, at a nominal resolution of 1.1 km.

Northern Saskatchewan is an area whose economy is closely tied to the forestry industry. Therefore, the early detection and location of forest fires is of vital importance for forest managers. Previous work has indicated the potential for using NOAA AVHRR data for the detection of hot spots such as gas flares and fires. The feasibility of forest fire detection using NOAA AVHRR channel 3 is examined in Part 3 of this Report. Limitations on the application of these data are examined. This is accompanied by a detailed methodology (Appendix) which outlines the procedure required for the detection of forest fires using this technology.

Part 4 of this Report contains conclusions drawn from Parts 2 and 3. Recommendations are also made with respect to the application of these technologies to ongoing climatological assessment, and to operational forest fire detection.

PART 2:

CLIMATE IMPACTS DETECTION IN SOUTHERN SASKATCHEWAN USING NOAA AVHRR DATA

INTRODUCTION

Despite advances in agricultural science and practice, climate remains a key variable in the vigour of crop and range vegetation, which comprises the majority of land cover in southern Saskatchewan (Richards, 1969). The growth of cereal crops and range vegetation is well suited to the prevailing climate in this region, but, as in most semi-arid areas, variability of precipitation during the critical growing season is the norm (Villimow, 1970), and is reflected in changes in the vigour of vegetation on a year to year basis. The refinement of techniques to monitor vegetation vigour in terms of precipitation variations using remote sensing, over an area as large as southern Saskatchewan, would be advantageous.

Multispectral remote sensing has proven to be very useful in assessing the vigour of plant cover at a point in time. Data analysis techniques have been in development since at least 1973. Rouse et al. (1973) developed one of the first successful vegetation indices based on band ratioing of Landsat MSS band 7 and band 5, by computing the normalized difference of band radiances. Tucker (1979) performed a similar analysis using photographic techniques in the red and near infrared regions of the spectrum, and found strong correlations between normalized indices and green leaf biomass. Wiegand et al. (1983), in an examination of drought detection and quantification using multispectral techniques, discusses the logic behind the vegetation index. Within the reflective wavelength region of the spectrum (0.4-1.35 μm), two relevant intervals are of note: the visible (0.4-0.75 μm), affected mainly by leaf chlorophyll content; and the reflective near infrared (0.75-1.35 μm), where leaf structure is important. They note that leaves that develop under stress such as drought have fewer air spaces in the leaves, and thus are less reflective in the near infrared than the unstressed leaves. Differences were noted in the field, but the magnitude of difference may be affected by amount of sunlit soil in the IFOV, planting configuration, soil wetness, atmospheric conditions, sun and sensor angles, and plant architecture. They conclude their discussion by noting that the most effective relationships were determined for the visible red (0.65 μm), far red (0.75 μm) and reflective infrared (0.90-1.10 μm) regions, so sensors which operate in these wavelengths will be most effective for evaluating drought's impact on vegetation.

As multispectral techniques were being developed to evaluate plant vigour, the advantages of the NOAA Advanced Very High Resolution Radiometer (AVHRR) system were being exploited. The NOAA AVHRR system provides high temporal resolution (2 times daily global coverage) which increases the likelihood of acquiring cloud free imagery over a large area during a critical biological "window", and it provides low spatial resolution (1.1 km at nadir), which is appropriate for subcontinental scales of analysis (Harris, 1985). The AVHRR sensor provides multispectral data in wavelengths appropriate for vegetation analysis (Harris, 1985). Specifically, AVHRR channel 1 is sensitive to the 0.58-0.69 μm range, and AVHRR channel 2 is sensitive to the 0.725-1.1 μm range (Allison and Schnapf, 1983). From these data a normalized difference vegetation index (NDVI) may be calculated as follows.

$$NDVI = \frac{\text{Channel 2 - Channel 1}}{\text{Channel 2 + Channel 1}}$$

The formula emphasizes differences between unstressed vegetation, which has a high reflectance in channel 2, and stressed vegetation, which has a low reflectance in channel 2.

The formula has been used with success by authors who examined green leaf biomass as revealed by the NDVI or its variants (eg. Tucker and Gatlin, 1984; Westlin et al., 1986), and has been employed in Canada by others (eg. Brown et al., 1982; Prout et al., 1986). Prout et al.(1986) examined the AVHRR NDVI and its relation to cumulative precipitation at climate

Figure 1. Study area showing crop district boundaries and precipitation stations.

stations in southern Saskatchewan. The relationship was promising, but was limited by the scope of the study (three locations examined), and so may be strengthened by broadening the analysis to include all of southern Saskatchewan and the primary climate observing stations therein.

The purpose of this Report is to examine the NDVI/precipitation relationship proposed by Prout et al. (1986). NDVIs were calculated on a pixel by pixel basis for the whole agricultural region of southern Saskatchewan (the study area is shown in Figure 1), and compared to cumulative precipitation during the growing season for the same area. Variance in NDVI not explained by precipitation may be due to: the influence of land management practices; year to year differences in crop heading dates; and any factors other than cumulative precipitation during the growing season, such as direct evaporation from the soil, antecedent soil moisture, pests, etc., which affect vegetation vigour.

METHODOLOGY

Local area coverage (LAC) AVHRR data, having approximately 1.1 km resolution at nadir, was obtained for five dates from four years. The images acquired were: July 19, 1983; July 26, 1984; July 19, 1985; June 14, 1986; and August 3, 1986. Prout et al. (1986) indicated that southern Saskatchewan vegetation experiences a "greenness wave", such that AVHRR-derived vegetation indices increase through time until they reach a peak which corresponds to crop heading, which occurs in mid to late July. For this reason, data were chosen in order to obtain such imagery under clear skies with the study area near nadir whenever possible. These criteria were satisfied in most cases. In the July 26, 1984 image, the study area is near swath edge, allowing only partial coverage. The June 14, 1986 image was chosen due its remarkable absence of cloud over the study area.

Following acquisition, preprocessing was performed to prepare the imagery for analysis. Geometric rectification was performed by registering each image to a previously corrected image with appropriate coverage. Registration was performed to the sub-pixel level (ie. standard error estimates in the line and pixel directions of less than 1000 m), and the data were resampled in 1 km pixels. Each image was adjusted for atmospheric effects by subtracting the minimum digital number found for large, turbidity-free lakes, found in northern Saskatchewan, from bands 1 and 2. Scan angle corrections were not performed since previous work has indicated that subsequent ratioing effectively removes the effects of varying path length on atmospheric attenuation and scattering (Jensen, 1986). This was confirmed by observing the calculated indices for lakes, whose indices should not vary with scan angle.

Normalized difference vegetation indices were calculated on a pixel by pixel basis by applying the difference over sum formula. Standard gains and offsets were used by determining those appropriate for the 1983 image (gain: 145; offset: 31) and applying these to each image. Geographic reference was provided by overlaying digitized Crop Reporting District boundaries.

Training areas were established using the Crop District boundaries as guidelines; lakes and forests were excluded to avoid biasing the statistics with areas whose NDVIs would not be expected to change from year to year. Separate training areas were created for each image such that cloud covered areas were excluded. Statistics were extracted from every training area on each image, providing the mean NDVI for each District.

Precipitation data over the study area were extracted from the Environment Canada Publication "Climatic Perspectives - Monthly Summary" in order ensure that a standardized methodology may be timely in future "real time" updating. Monthly precipitation during the growing period and up to image dates (ie. April to image date) were used for

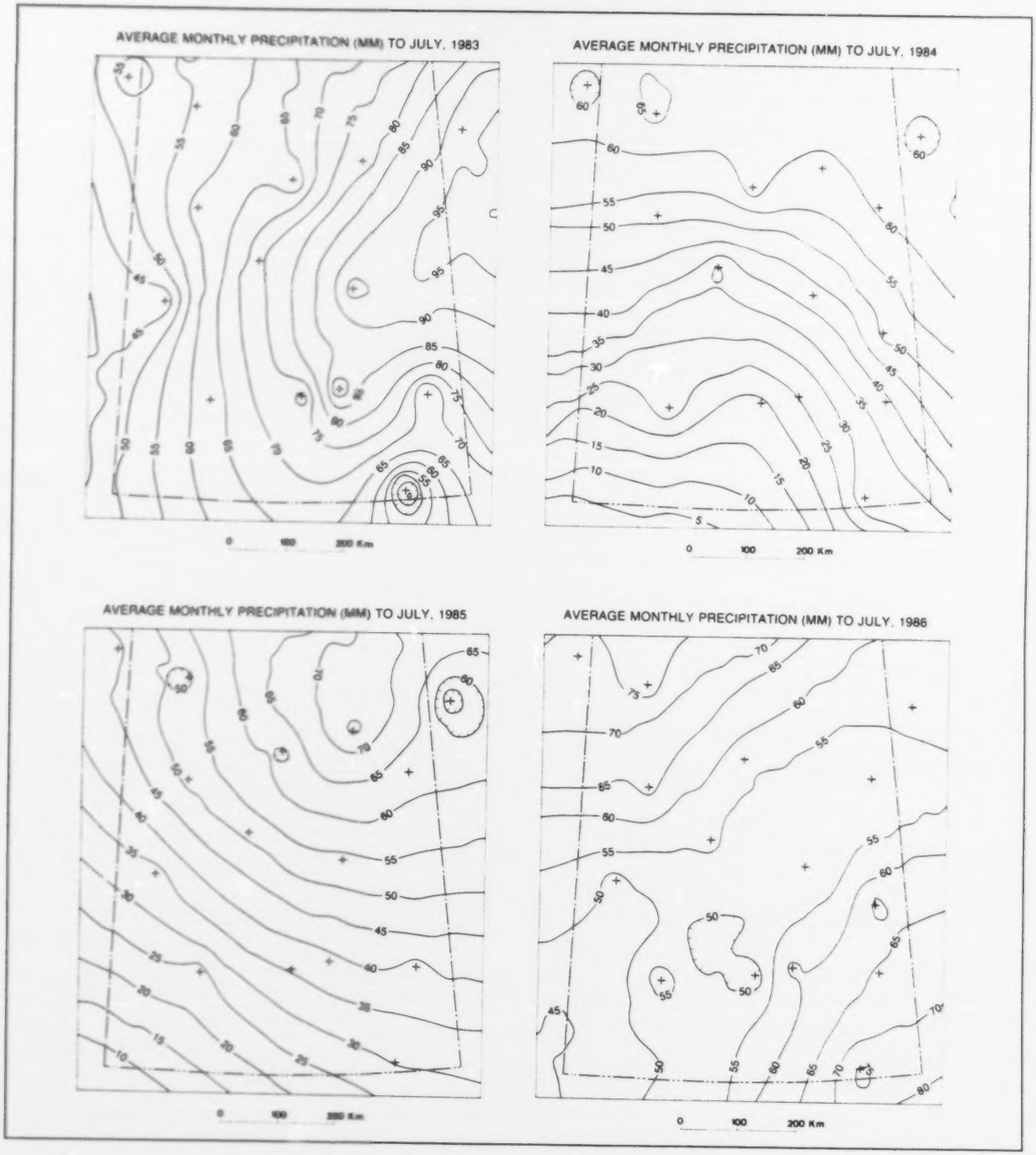
AVERAGE MONTHLY PRECIPITATION (MM) TO JULY, 1983
AVERAGE MONTHLY PRECIPITATION (MM) TO JULY, 1984
AVERAGE MONTHLY PRECIPITATION (MM) TO JULY, 1985
AVERAGE MONTHLY PRECIPITATION (MM) TO JULY, 1986
0 100 200 Km

Figure 2. Average monthly precipitation to July in each of the four Test Years.

each of the 20 Saskatchewan stations and 4 stations immediately adjacent to Saskatchewan. These data were plotted (Figure 2) and were subsequently sampled by overlaying the Crop District boundaries.

In this manner, mean NDVI and precipitation data are available for each of 19 geometric regions within the study area. These data are shown in Table 2, and are discussed in the following section.

PART 2:

TABLE 2
NDVI AND PRECIPITATION DATA BY AREA

AREA	MEAN PRECIP (mm)				MEAN NDVI				
	1983	1984	1985	1986	1983	1984	1985	1986 June	1986 Aug.
1A	54	50	45	67	159	144	115	114	160
1B	50	40	35	51	127	114	110	93	147
2A	51	31	30	49	124	104	105	86	131
2B	70	32	40	52	143	102	118	99	138
3AN	81	40	55	53	165	129	144	94	147
3AS	81	28	42	51	146	102	129	99	138
3BN	53	21	22	47	96	82	89	98	120
3BS	63	26	24	55	114	86	101	99	124
4A	53	10	14	47	94	77	88	121	119
4B	70	16	30	52	123	84	101	104	122
5A	69	12	25	62	109	98	107	123	110
5B	71	20	32	62	151	na	108	101	139
6A	60	28	32	72	192	na	122	107	147
6B	68	35	37	66	139	na	108	135	138
7A	80	21	35	60	135	na	124	91	124
7B	61	11	17	51	106	79	86	105	110
8A	80	38	43	62	163	na	144	103	146
8B	90	45	50	58	184	na	150	105	155
9B	92	55	58	53	196	na	153	126	157

notes:
1. NDVI: Normalized Difference Vegetation Index
2. na: not available due to lack of image coverage
3. see figure 1 for area locations

DISCUSSION

Figure 3 is scatterplots of the average NDVI and precipitation by Crop District. Examination of these, and the Pearson correlation coefficients which were calculated in each case, gives an indication of the strength of the relationship between mean NDVI and mean precipitation by District in five cases. Reasonable correlation was found in all but one of the cases. The lowest correlation (r=0.18) was found for the June 14, 1986, which was during the growing season, but not near crop heading. Because of this poor relationship, and because a later image was available for 1986, this image was not used in subsequent analysis. The results do indicate, however, the importance of the selection of images with similar dates near heading for comparative vegetation analysis.

Further analysis of remaining cases showed that better relationships were found for years with below normal precipitation. The precipitation means and ranges over the study area are noted in Table 3. The two drier years amongst the cases, 1984 and 1985, had correlation coefficients of 0.84 and 0.91 respectively, whereas the two wetter years, 1983 and 1986, had coefficients of 0.57 and 0.43 respectively. Considering extraneous factors which may affect NDVIs, the relationships are reasonable, and, significantly, become stronger during "droughty" years

TABLE 3
Precipitation and Correlation Statistics for Study Area

YEAR	MONTHLY PRECIPITATION (mm)			r
	MEAN	MAXIMUM	MINIMUM	
1983	68.3	92.0	50.0	0.57
1984	29.4	55.0	10.0	0.84
1985	35.1	58.0	14.0	0.91
1986	56.3	72.0	47.0	0.43

The data from all years was combined to determine if absolute values of NDVIs are related to precipitation. A combined correlation coefficient of 0.77 was found; the scatterplot is depicted in Figure 4 on which a least squares best fit line is shown. The coefficient shows that, even considering the relatively poor relationship exhibited in "wet" years, the data exhibit colinearity, showing that the absolute NDVIs strongly reflect precipitation patterns and magnitudes. This was confirmed by normalizing the data; that is,

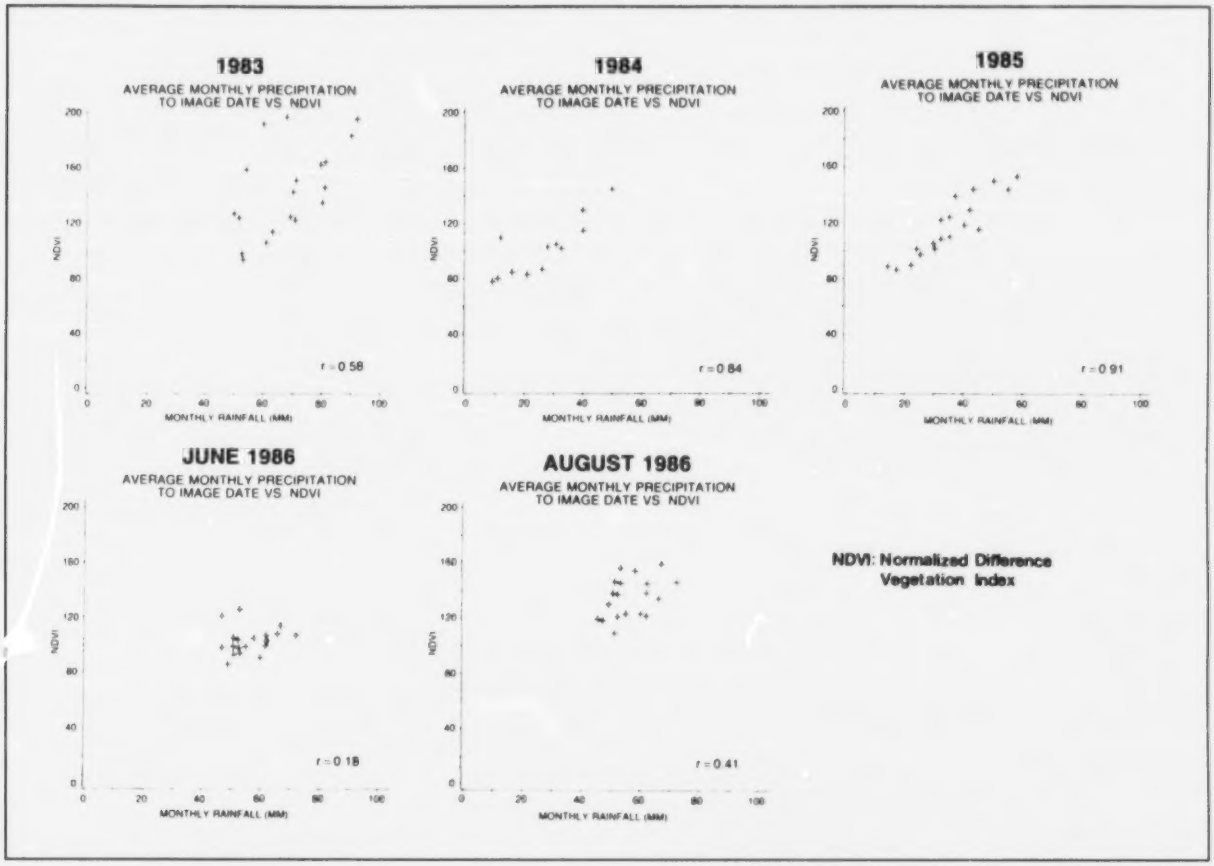

Figure 3. The normalized difference vegetation index (NDVI) as a function of monthly rainfall for each test period.

using 1983 as an arbitrary standard to which other cases may be compared, NDVI differences were compared to precipitation differences by area. This removed the effect of precipitation on NDVI; any remaining variation would be due to other factors. This is shown in Figure 5, and the very low correlation coefficient of -0.09 confirms the expected lack of correlation.

CONCLUSION

The study has shown that the proposed relationship between AVHRR NDVIs calculated on a pixel by pixel basis over the agricultural region of southern Saskatchewan, and precipitation, is a valid one. Precipitation explained the majority of variance in mean NDVI; the relationship was weakest in wet years, and strengthened in dry years. Further, analysis of an early (June) image showed the importance of choosing similar image dates, or dates at similar points in the growing season, for comparison on a year to year basis.

The absolute value of the NDVI is shown to be positively correlated to precipitation by area. This allows comparisons between years as well as within years. Also, it shows the potential for the preparation of a "normal" NDVI image to which any year's image could be compared using image differencing techniques. Such a comparison would show the location and magnitude of variations in vegetation vigour on a pixel by pixel basis at a point in time.

The relationship is a strong one for the study area examined. Southern Saskatchewan is largely semi-arid; any input of moisture during the growing season will likely have a positive impact on vegetation vigour, producing a linear relationship. Significantly, the effect is weakened in wetter years, when vegetation is not as impacted by a lack of moisture. One would therefore expect this relationship to hold only in areas which normally have a negative soil moisture balance. The global occurrence of such areas is indicated by the incidence of "B" (dry) climates in Koppen's classification (Briggs and Smithson, 1985) as shown in Figure 6.

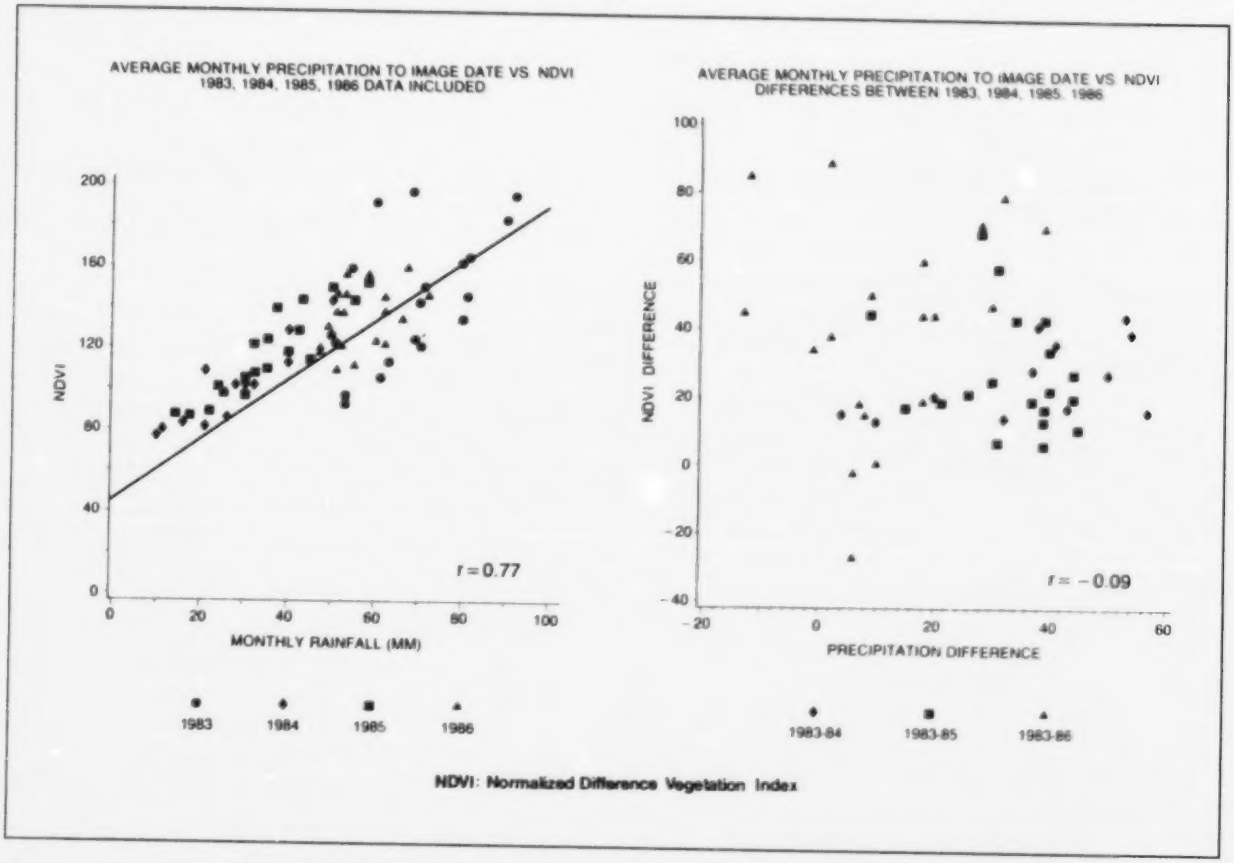

Figure 4. NDVI as a function of monthly rainfall for all four years.

Figure 5. NDVI differences (from 1983 data) plotted against precipitation differences for the same years.

Previous work has shown the utility of the AVHRR NDVI for monitoring vegetation condition over large areas. This study has shown that the index is valid under a variety of data acquisition conditions (i.e. four separate years) over the agricultural area of southern Saskatchewan. It has also shown that the majority of variance in vegetation vigour is controlled primarily by precipitation during the growing season, a relatively simple variable.

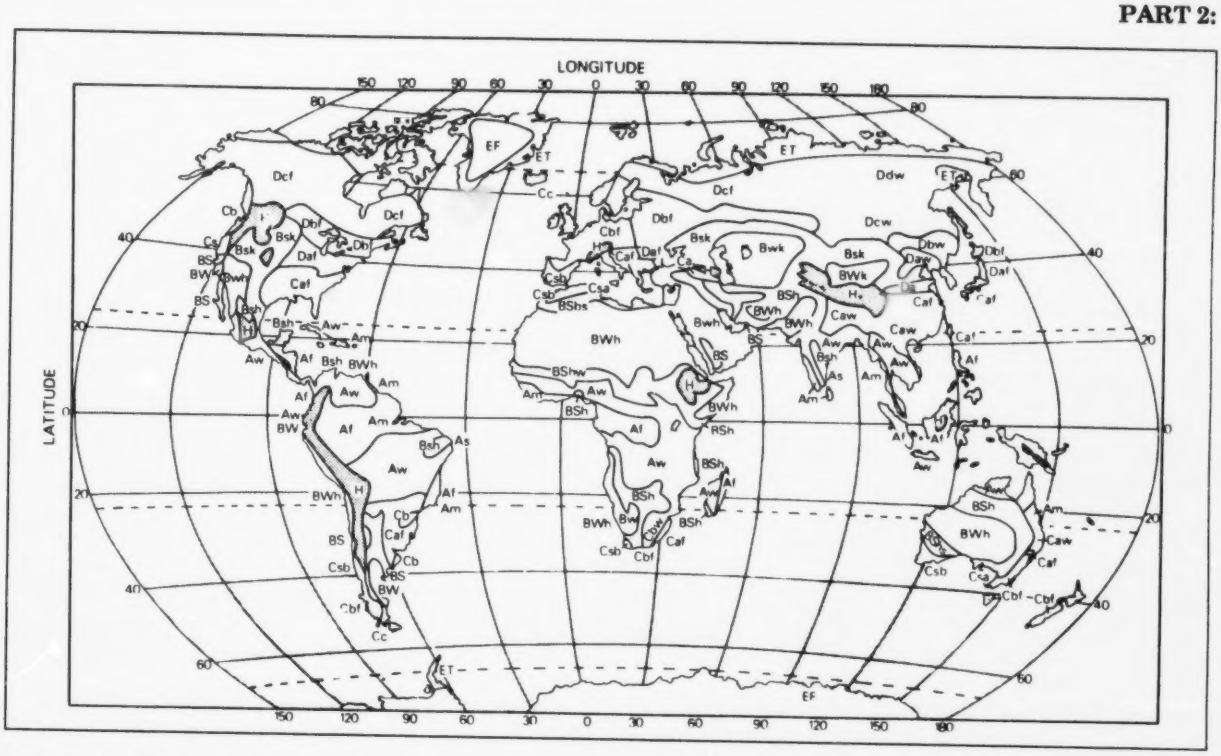

Figure 6. Climates of the continents according to the Koppen Classification. Areas with negative soil moisture budget have a "B" designation (from Briggs and Smithson, 1985).

PART 3:

FOREST FIRE DETECTION IN NORTHERN SASKATCHEWAN USING NOAA AVHRR CHANNEL 3 DATA

INTRODUCTION

Several recent studies (eg. Matson et al., 1984; Matson et al., 1985; and Matson and Stephens, 1985) have suggested that NOAA AVHRR data would be of great benefit to the operational early detection of forest fires. This Part of the Report will examine the potential use of these data for fire detection in northern Saskatchewan. The logic of this use will be examined, accompanied by a discussion of limitations of previous studies on this topic. The Saskatchewan situation will be examined through a case study approach, in which several images are analysed in order to detect potential fires, and these data are compared to the incidence of known fires on appropriate dates. In this way, a methodology for forest fire detection using NOAA AVHRR data may be determined, accompanied by an outline of shortcomings and limitations of the technology.

Hirsch (1964, from Heller and Ulliman, 1983) lists the attributes of an ideal forest fire detection system:

a) fire detection at instant of start;
b) effective day and night operation;
c) operation in low visibility conditions such as smoke, fog, or dense timber cover; and
d) ability to differentiate potentially dangerous fires from those of no concern to fire control forces.

Attribute (a) necessitates a system with sufficient spatial resolution to detect small fires, with coverage of high temporal frequency, and with area of coverage sufficient to survey the area of interest. Attribute (b) precludes the use of the visible range; thus restricting attention to thermal infrared systems. This means that more than the smoke plume must be found; smoke plume detection requires solar illumination (see eg. Chung and Le, 1984). We turn our attention to the applicability of the NOAA AVHRR system, especially channel 3, which responds to high temperature sources, to the problem.

Matson and Dozier (1981) examined the use of the AVHRR Channel 3 (see Table 1) for detecting high temperature sources. Matson and Dozier found when comparing the pixel by pixel response of channels 3 and 4 (each of them being thermal IR channels), their responses were unequal for high temperature sources, channel 3 giving a higher brightness temperature. This observation is explained by Figure 7, which shows Planck radiances for temperatures from 200 K to 500 K. Matson et al. (1984) state that for a given increase in temperature, the increase in area under the channel 3 segments of the curves is much greater than under the channel 4 segments. This means that, for high temperature sources, the response in channel 3 will be greater than that in channel 4.

Matson and Dozier (1981) state that for pixel-sized sources, channel 3 will saturate at a brightness temperature (which is less than the thermodynamic surface temperature of the source by emissivity and attenuation factors) of 321 K. Many hot sources (such as gas flares) occupy only a very small portion of the (minimum) 1.1 km pixel and therefore may not saturate channel 3. Whether it saturates or not depends on: the radiant temperature of the source; the actual size of the source; the actual pixel size (which may be larger than 1.1 km in the across-track direction if away from nadir); and the occurrence of atmospheric attenuation in channel 3's spectral response range (especially by clouds). Gorham (pers. comm., 1987) indicates that the thermodynamic temperature of forest fires is at least 350 C (623 K) and that of open flame may exceed 1200 C (1473 K). This fact increases the likelihood of even subresolution sources saturating channel 3 pixels. Matson and Dozier (1981) note that such saturation will be confined to individual pixels; there will be no "spill-over" effect into adjacent pixels.

Matson and Parmenter-Holt (1985) indicate that high temperature sources which saturate channel 3 (at whatever size and thermodynamic temperature) will appear as white or black "hot spots" on the image, depending on preprocessing and display enhancements used. With 8 bit digital data, these "hot spots" will be pixels with a digital number (DN) of either 0

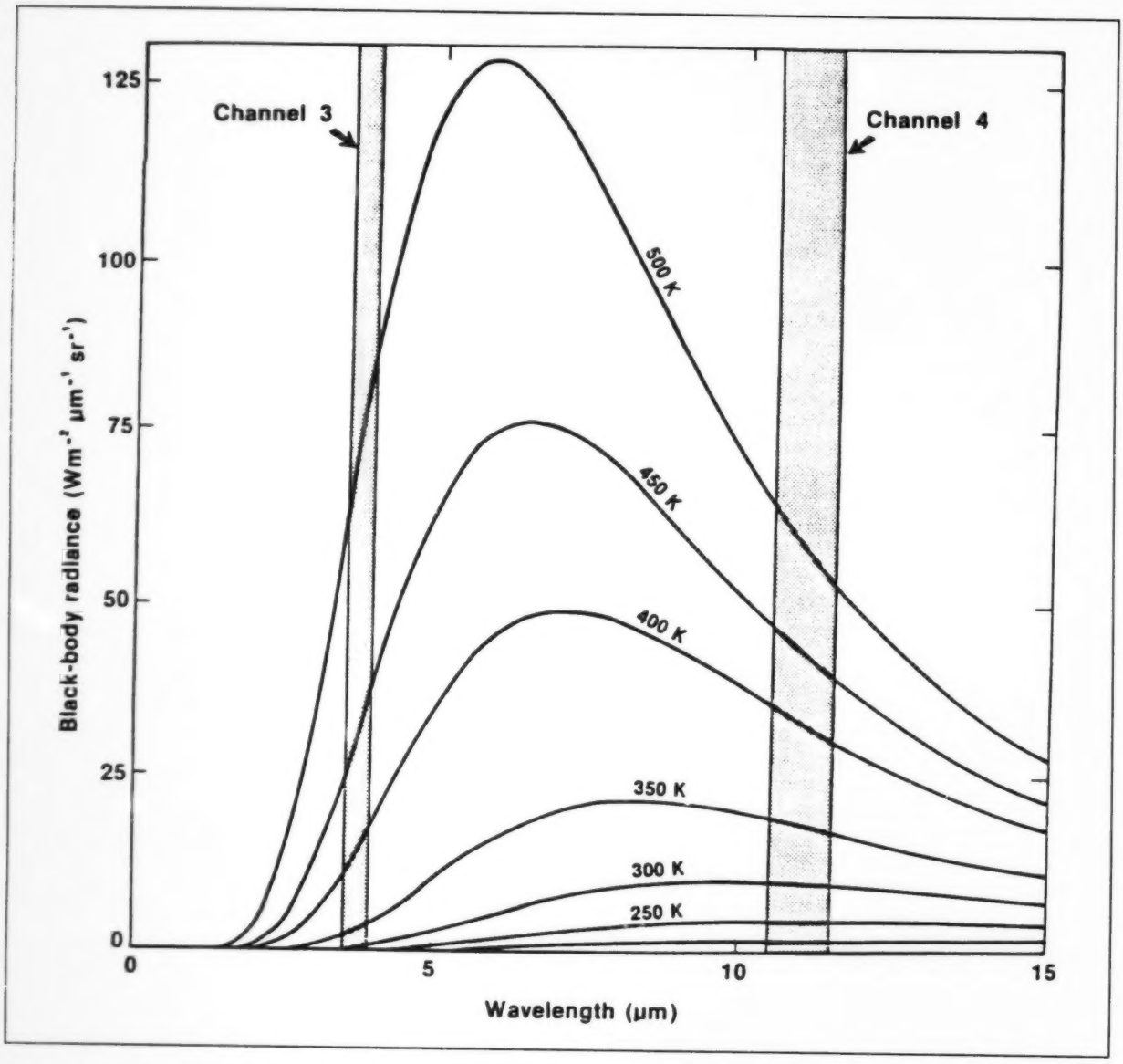

Figure 7. Planck radiances for temperatures from 200 K to 500 K. For a given increase in temperature, the increase in area under the channel segments of the curves is much greater than under the channel 4

or 255. High temperature sources which do not saturate the channel will nonetheless strongly affect its response, so the hot spots will likely have DN's quite close to one of these values.

In summary, recent studies have pointed out the potential application of NOAA AVHRR data for the detection of forest fires. The logic of this potential has been well documented, and was briefly reviewed here, but there is a lack of discussion of specific methodologies, and of limitations of this technology. These are addressed with reference to Saskatchewan examples, in the remainder of Part 3.

METHODOLOGY

The feasibility, methodology, and limitations of forest fire detection using the NOAA AVHRR system were investigated through a case study approach, in which forest fire occurrences and locations as detected by remote sensing means were compared to forest fires of known occurrence and location. Four NOAA AVHRR images, having northern Saskatchewan coverage were obtained for analysis from the Canada Centre for Remote Sensing through its Technology Enhancement Program. Image dates

TABLE 4
FOREST FIRE LOCATIONS AND SIZES

ID #	Start Date	Out Date	Start Size (ha)	Out Size	UTM Easting	UTM Northing
(On June 14, 1984)						
846059	06/14	07/01	0.01	0	569000	6194000
848021	06/14	06/17	.3		682500	6196000
848018	06/14	16/19	2	3	670500	6307500
848019	06/14	06/20	.09		665000	6311000
848407	06/14	06/21	4	7	352000	6264500
846036	06/14	06/23	5	15	485000	6274000
846803	06/14	07/09	2	12150	430000	6262000
846027	06/14	06/20	7	70	435000	6262000
846603	06/14	06/16	2.5	5	444000	6487000
846602	06/14	06/16	3.5	4	447000	6489500
846032	06/14	06/16	0.4	0	542500	6240000
846031	06/14	06/18	0.4	0	533000	6517500
846502	06/14	06/23	20	325	618000	6517500
(On July 26, 1984)						
847130	07/25	07/27	.02		582500	6179000
847129	07/25	07/28	2	3	583200	6184000
847132	07/25	08/04	2	10	583000	6164000
848222	07/26	08/13	150.0	5060	331500	6378000
846139	07/26	08/21	20	858	662500	6272000
(On July 3, 1985)						
85L717	07/01	07/10	1.0	1	408000	6660000
85CA57	07/01	07/12	1.0	130	413000	6394000
85L711	07/01	08/05	3	108	508000	6613000
85L710	07/01	08/10	.1	990	498000	6603000
85L714	07/01	08/04	.5	28360	405000	6644000
85L604	07/01	08/15	100.0	13120	604000	6507000
85L726	07/02	07/12	10.0	11	464000	6633000
85L712	07/02	07/11	5	10	470000	6637500
85L713	07/02	07/06	5.0	13	432500	6622500
85CB13	07/03	07/10	25	41	671000	6435000
85L715	07/03	07/06	1.0	48	454000	6534000
85L716	07/03	07/05	1.5		662000	6597000

were chosen so that several fires of known size and location, as indicated by Gorham (1986), were burning at the time of satellite overpass. The four images acquired were:

1) June 14, 1984
2) July 26, 1984 AM
3) July 26, 1984 PM
4) July 3, 1985

These images were pre-processed at the Prince Albert Satellite Receiving Station prior to acquisition, such that in channel 3, hot targets have a dark signature (low DN). This is done in order that high clouds, which are cold, appear white.

Also acquired was information pertaining to the location and size of fires known to be burning in northern Saskatchewan at time of image acquisition, provided by the Saskatchewan Forest Fire Management Office of Saskatchewan Parks, Recreation and Culture (SPRC). This information is shown in Table 4.

Following image acquisition, CCT data were read to disk for subsequent digital analysis. Image subareas were created in each case providing northern Saskatchewan focus and reduction of image processing time. Dropped lines were replaced for cosmetic purposes using the average of the preceding and following lines. For images acquired on the ascending pass of the satellite, rotations were performed to put north near the top of the image. Images were resampled using the nearest neighbour method (the logic of this decision is addressed later herein). The images were geometrically registered to the Univer-

Figure 8. An example of forest fire detection from a specific satellite image.

sal Transverse Mercator (UTM) coordinate grid by performing image-to-image registration on a previously corrected image. The nearest neighbour method of resampling was again used.

Density slicing was performed on each image's AVHRR channel 3. In each case, two classes were created from channel 3 such that the first class represented DN's ranging from 0 to 1, and the second class from DN 2 to 9. Therefore, the first class represents those channel 3 pixels which were saturated by hot sources, whereas the second class represents those pixels which were very strongly affected by hot sources (but saturation did not occur). Further density slicing was performed using channel 2 (the near IR channel). A class was created which represented water areas to provide geographic reference. Another class was created which represented cloud covered areas. In the density slicing of channel 2, each image was evaluated separately in order to determine slicing levels appropriate to each; these are variable due

to the differing effects of atmospheric absorption and scatter, and different cloud characteristics, between images.

A 50 kilometre UTM grid overlay was created to provide further geographic reference. Ink-jet plots were created of each density-sliced image at a scale of 1:6,000,000.

As a result of the previous operations, for each case a plot was produced with five classes: lakes; cloud covered areas; a 50 km UTM grid; pixels which saturated under the influence of hot sources ("true" hot spots); and pixels which were strongly influenced by the effect of hot sources, but did not saturate ("potential" hot spots). (An example plot, showing the density slice classes determined for a segment of the July 3, 1985 image, is shown on the following page in Figure 8. Each fire of known location and size as shown in Table 1 was compared to the plot for the appropriate image. The results of this analysis are discussed below.

In addition to the image processing described above, the analysis was repeated with the following difference. Whenever resampling was performed, it was accomplished using the cubic convolution method instead of the nearest neighbour method. Results of the use of these two methods were compared and are also discussed below.

DISCUSSION

For each of the fires described in Table 4, its position was found on the appropriate ink-jet plot showing lakes, clouds, true hot spots and potential hot spots. In this way, the occurrence of known fires could be compared to fires detected by the method described above. The plotting of cloud covered areas allows the possible explanation of nondetection of actual fires. The results of this analysis is shown in Table 5.

Examination of Table 5 reveals the following:

a) The occurrence of cloud prevents the detection of surface fires. This is in contradiction with Matson and Parmenter-Holt (1985), who state that channel 3 "penetrates" smoke and cloud to reveal the fire areas. It is suggested here that fires detected "through" clouds and smoke are actually the result of hot smoke particles and gases being detected by channel 3. In the present study, this occurred in the case of fire 85L604.

b) When actual fires occur near the edge of the image swath, they are not likely to be detected, unless the fire is 5-8 km in size or of high temperature. Pixel size changes as a result of varying scan angle are significant on the AVHRR sensor. Pixel size is a minimum of 1.1 km at spacecraft nadir, and increases toward swath edge.

c) No clear relationship exists between actual fire size and fire size as detected by the AVHRR system. The only generalization that may be made is that the system consistently overestimates fire size. The minimum size of fire detected by SPRC was 0.09 ha (fire 848019). Detection size by NOAA AVHRR of this fire was at least 121 ha (1 pixel).

d) Examination of fires 85CB13 and 85L715 reveals an apparent contradiction. The actual size of the former was 25 ha and the detection size was 121 ha (1 pixel), while the actual size of the latter was 1 ha and the detection size was 726 ha (6 pixels). A possible explanation of this lies in the growth of the fire since detection by conventional means. Fire 85L715 was detected by conventional means on July 3, 1985 when it was 1 ha, but it grew quickly to a final size of 48 ha, making the actual size at time of satellite detection difficult to estimate. In contrast, fire 85CB13 was detected by conventional means when it was 25 ha, and it grew slowly to a final size of only 41 ha suggesting that 25 ha is a reliable estimate of its size at time of satellite detection.

As noted earlier, supplemental analysis was carried out to test the efficacy of different resampling methods when image rotation or geometric rectification is performed. Resampling is the process by which the original image with line and pixel coordinates is transformed to a new coordinate system (Curran, 1985). The two methods performed were nearest neighbour, and cubic convolution. Curran (1985) discusses these resampling methods, and discusses their characteristics In cubic convolution resampling, the new pixel DN is a weighted average of that of the nearest 16 pixels. This results in a very "smooth" image, and for this reason it is the preferred method for most applications. However, this method alters the data set (ie. the DN is altered). In nearest neighbour resampling, the new pixel DN is simply a transfer of the DN of the nearest pixel in the original data set. The disadvantages of this method are that it results in a "disjointed" image, and that pixels may displaced by up to half a pixel. However, DNs are unaltered, which retains the radiometric characteristics of the original data set.

Although the data from this analysis are not presented here, the results may be summarized briefly. Fires were detected with greater consistency when the nearest neighbour method was used. When using the cubic convolution method, a new data set with

PART 3:

TABLE 5
COMPARISON OF KNOWN FIRES WITH DETECTED FIRES

ID #	SPRC FIRE SIZE (ha)	NOAA HOT SPOT (ha)	NOAA WARM SPOT (ha)	COMMENTS
(On July 14, 1984 image)				
846059	0.01	na		obscured by cloud
848021	0.3	na		" " "
848018	2	0	121	
848019	0.09	0	121	
848407	4	na		" " "
846036	5	na		" " "
846803	2	na		" " "
846027	7	na		" " "
846603	2.5	na		" " "
846602	3.5	na		" " "
846032	0.4	na		" " "
846031	0.4	na		" " "
846502	20	na		" " "
(On July 26, 1984 images)				
847130	0.02	na		at image edge
847129	2	na		" " "
847132	2	na		" " "
848222	150	na		obscured by cloud
846139	20	na		no image coverage
(On July 3, 1985 image)				
85L717	1	na		no image coverage
85CA57	1	0	1089	2 days old
85L711	3	0	2420	2 days old
85L710	0.1	na		obscured by cloud
85L714	0.5	na		no image coverage
85L604	100	1573	7865	2 days old
85L726	10	na		no image coverage
85L712	5	na		no image coverage
85L713	5	na		not detected
85CB13	25	0	121	---
85L715	1	0	726	---
85L716	1.5	na		not detected (perhaps not started at satellite overpass)

radiometric characteristics different from the original is created. Averaging is performed which "smooths out" pixels with DNs significantly different from their surroundings. In the case of fire detection, small subresolution sources are of particular interest, so it is important to use the nearest neighbour method whenever resampling is done so that isolated, saturated pixels are preserved.

CONCLUSION

The preceding discussion shows that considerable success was gained in the case study analysis of forest fire detection using relatively simple density slicing of NOAA AVHRR digital data. As worthwhile as the demonstration that fires can indeed be detected and located, is the gleaning of limitations and constraints of this technology. Conclusions drawn from this study may be summarized as follows:

The satellite sensor system and data analysis techniques are capable of detecting and locating even subresolution forest fires. This detection, being thermally rather than visually based, is not dependent on solar illumination, so there is a day and night capability. Hirsch (1964) had indicated that this is a desired attribute of an "ideal" fire detection system.

The detection of forest fires using AVHRR channel 3 is significantly limited by:

a) Clouds which obscure existing fires. Clouds are efficient absorbers of infrared radiation, which is the type of radiation detected by AVHRR channel 3.

b) Coverage of area of interest near image swath edge. The spatial resolution of the NOAA AVHRR system is strongly dependent on scan angle. Since the actual pixel size becomes large near swath edge, the forest fire would have to be larger or hotter to be detected.

Of those fires not obscured by cloud, 58% were detected by NOAA, with a further 25% located near the swath edge. This means that only 17% of "detectable" fires were not detected. Thus, in order for fires to be reliably detected, two significant constraints must be placed on data acquisition. First, the area of interest must be relatively free of cloud. Absolute cloud free conditions are neither realistically expected nor necessary. Several of the actual fires were detected in areas with partial cloud cover. Second, the area of interest should be within 45 of image swath centre. This keeps the pixel size near minimum, and increases the likelihood of detecting subresolution fires.

No clear relationship has been found to exist between actual fire size and detected fire size, except for the obvious observation that the system consistently overestimates actual size. Thus, it is not recommended that this system be used to estimate the size of affected or burning areas.

A comparison of resampling algorithms which are used when geometric correction or image rotation is performed has shown that the nearest neighbour method is preferred. This method preserves the radiometric characteristics of the original data set. For the purpose of thermal detection of forest fires, the radiometric characteristics of affected pixels are of paramount importance.

The study has shown that, under constrained conditions, NOAA AVHRR channel 3 is capable of detecting even subresolution forest fires. The importance of choosing the appropriate resampling algorithm, nearest neighbour, has been illustrated. Thus, the application of these data and data analysis methods shows considerable potential for supplementing present fire detection procedures. Although the constraints on this technology prevent the replacement of present methods, its application would very likely result in the early detection and location of many forest fires which presently go unnoticed until they have burned large areas of valuable forest.

PART 4:

MAJOR CONCLUSIONS AND RECOMMENDATIONS

Parts 2 and 3 of this Report have described the rationale, methodologies, and results of the application of NOAA AVHRR data to two environmental or resource problems of importance to Saskatchewan. Part 2 outlined the applicability of these data to evaluating the vigour of vegetation in the agricultural region of Saskatchewan in terms of precipitation during the growing season. Part 3 investigated the potential for the detection of forest fires using these data. Success was obtained in each case. This Part will summarize the major conclusions drawn from these studies, and will outline recommendations for further study and/or the implementation of these data and data analysis techniques in an operational sense.

CONCLUSIONS

Major conclusions drawn from this study are listed below, with the discussion on which they are based being the appropriate sections in Parts 2 and 3 of this Report:

For Part 2 (Vegetation/Precipitation Assessment):

1) The study has validated the relationship proposed by others between a Normalized Difference Vegetation Index calculated from NOAA AVHRR channels 1 and 2, and precipitation during the growing season. The relationship had not been previously adequately tested in the semi-arid agricultural region of Saskatchewan.
2) The absolute value of the NDVI is positively correlated to precipitation. This illustrates the potential for comparing vegetation vigour between years (or images) as well as between places within the a single image. Such a comparison could be used to evaluate the magnitude of vegetation vigour changes between points in time, or between a point in time and a standard.

For Part 3 (Forest Fire Detection):

1) The NOAA AVHRR satellite sensor is capable, albeit under constrained conditions, of detecting even subresolution forest fires which are burning at the time of satellite data acquisition. The major constraints are listed below:
   a) The system is not capable of detecting fires when the high temperature source is obscured by clouds.
   b) The system is less capable of detecting fires which occur near the image swath edge.
   c) The system consistently overestimates actual fire size in a presently unknown manner.

2) Digital data resampling, performed whenever geometric corrections or image rotations are done, must be accomplished using the nearest neighbour method.
3) Implementation of the system would be a worthwhile supplement to present fire detection practise, due to its ability to detect, early, any small existing fires, and the four times daily coverage.

RECOMMENDATIONS

This Report has shown that specially enhanced NOAA AVHRR data is potentially beneficial for two separate resource analysis problems of interest to the people of Saskatchewan. The following recommendations are made with respect to the further development, testing, and implementation of this technology.

1) NOAA AVHRR data, acquired near crop heading date, should be obtained on an annual basis for summers subsequent to those analysed in Part 2 of this Report. The objectives of this acquisition are as follows:
   a)To continue to monitor the vigour of vegetation in southern Saskatchewan.

b)To build up an image library of NOAA AVHRR NDVI images so that an updatable "normal" NDVI image might be prepared. Such an image would provide a standard to which any given image could be compared. This would enable the delineation of areas which are positively or negatively affected using image differencing techniques.

2) A fire detection "trial run" should be performed. This would entail the acquisition and analysis of NOAA AVHRR channel 3 data followed by provision of information to the Fire Control Office. The objective of this exercise would be:

a)To determine if the system can provide information currently received by forest managers more quickly than at present.

3) Fire detection using the NOAA AVHRR system should be implemented as a supplement to current methods. This would necessitate the rapid transfer of satellite data to an image processing facility, or the establishment of image processing resources at the point of satellite data receipt. Care must be taken on an ongoing basis to obtain cloud free data with the area of interest at image swath centre.

In summary, the exploitation of NOAA AVHRR data shows considerable potential. The high frequency of large area coverage with appropriate spectral ranges makes this an attractive data source for environmental analyses. The studies reported here have shown that the utilization of these data for climate impact assessment and forest fire detection would be beneficial, and warrants further study or implementation.

REFERENCES

Allison, L.J., and A. Schnapf, eds., 1983. "Meteorological satellites" in Simonett, D.S. and F.T. Ulaby, eds. *Manual of Remote Sensing, Vol. 1* 2 ed. Amer. Soc. Photogrammetry, Falls Church, Va. pp.651- 678.

Briggs, D. and P. Smithson, 1985. *Fundamentals of Physical Geography* Hutchinson: London.

Brown, R.J., M. Bernier, G. Fedosejevs, and L. Skretkowicz, 1982. "NOAA AVHRR crop condition monitoring" *Canadian Journal of Remote Sensing* 8(2) pp.107-117.

Chung, Y.S., and H.V. Le, 1984. "Detection of smoke plumes by satellite imagery" *Atmospheric Environment* 18(10) pp. 2143-2151.

Curran, P.J., 1985. *Principles of Remote Sensing* Longman: Essex, Eng- land. p. 194.

Environment Canada *Climatic Perspectives - Monthly Summary* Atmospheric Environment Service, Downsview.

Gorham, K., 3 Oct., 1986. pers. comm., Saskatchewan Forest Fire Manage- ment Office, Prince Albert, Saskatchewan.

Harris, R., 1985. "Satellite remote sensing: low spatial resolution" *Progress in Physical Geography* 9(4) pp.601-606.

Heller, R.C., and J.J. Ulliman, eds., 1983, "Forest Resource Assessments" in J.E. Estes and G.A. Thorley, eds., *Manual of Remote Sensing, 2 ed., Vol. II: Interpretation and Applications* Falls Church, Va.: Amer. Soc. Photogrammetry. pp. 2229-2324.

Hirsch, S.N., 1964, "Forest fire detection systems" *Western Forest Fire Research Council, Proceedings, 1964.* pp. 3-5.

Jensen, J.R., 1986. *Introductory Image Processing: The Remote Sensing Perspective* Prentice-Hall, Englewood Cliffs, N.J.

Matson, M. and J. Dozier, 1981. "Identification of subresolution high temperature sources using a thermal IR sensor" *Photogrammetric Engineering and Remote Sensing* 47(9), pp. 1311-1318.

Matson, M. and F. Parmenter-Holt, 1985. "Hydrologic and Land Sciences Applications of NOAA Polar-Orbiting Satellite Data" U.S. Dept. of Commerce, Washington D.C. 19 pp..

Matson, M., S. Schneider, B. Aldridge, and B. Satchwell, 1984. "Fire detection using the NOAA - series satellites" *NOAA Technical Report NESDIS 7.* U.S. Dept. of Commerce, Washington D.C.. 34 pp..

Matson, M. and G. Stephens, 1985. "Fire detection using NOAA polar- orbiting satellite data" *in Pecora 10: Proceedings, Remote Sensing in Forest and Resource Management, Aug. 20-22, 1985, Colorado St. University.* Amer. Soc. Photogrammetry and Remote Sensing, Falls Church, Va. p. 445.

Prout, N.A., et al., 1986. "Technological feasibility to mobilization for operations: the NOAA crop monitoring case" *Proceedings, 10th Canadian Symposium on Remote Sensing, May 5-8, 1986* Edmonton, Alberta. pp.787-796.

Richards, J.R., ed., 1969. *Atlas of Saskatchewan* Modern Press, Saskatoon.

Tucker, C.J., 1979. "Red and photographic infrared linear combinations for monitoring vegetation" *Remote Sensing of Environment* 8(2) pp.127-150.

Tucker, C.J., and J.A. Gatlin, 1984. "Monitoring vegetation in the Nile Delta with NOAA-6 and NOAA-7 AVHRR imagery" *Photogrammetric Engineering and Remote Sensing* 50(1) pp.53-61.

Villimow, J.R., 1970. "The nature and origin of the Canadian Dry Belt" in J.G. Nelson et al., eds. *Weather and Climate: Selected Readings* Methuen, Toronto. pp.51-74.

Westlin, F.C., D.O. Ohlen, and D.G. Moore, 1986. "Using AVHRR data to evaluate the greenness variability within monitoring polygons" *Proceedings, 10th Canadian Symposium on Remote Sensing, May 5-8, 1986* Edmonton, Alberta. pp.265-271.

Wiegand, C.L., P.R. Nixon, and R.D. Jackson, 1983. "Drought detection and quantification by reflectance and thermal responses" *Agricultural Water Management* 7 pp.303-321.

ACKNOWLEDGEMENTS

The author would like to acknowledge the following persons and organizations: R. Brown and J.C. Henein of the Canada Centre for Remote Sensing provided NOAA imagery, for which the author is grateful. Thanks also to K. Gorham of the Saskatchewan Forest Fire Management Office, who provided control data, and to D. Epp of SED Systems who suggested implementation of the forest fire study. CCRS provided image analysis support through its Technology Enhancement Programme. The study was funded by the Saskatchewan Research Council. Many thanks to H. Epp of CCRS and J. Whiting of SRC who provided valuable advice and guidance.

APPENDIX

METHODOLOGY

Step-by-step methodologies are provided here, in order that subsequent analyses may be undertaken by analysts other than the author with a minimum of difficulty. The methodologies given assume access to a Dipix Aries image analysis system (ie. task names and file naming conventions given are unique to that system). When specific file and/or tape names are given, they may be found in the Saskatchewan Research Council Remote Sensing tape library.

FOR PART 1 (Climatic Assessment)

1. Data Acquisition. Acquire NOAA AVHRR data with geographic coverage of southern Saskatchewan, with the study area near image swath centre. Ideally, the study area should be cloud free, although it is perhaps more important that the image date is near crop heading (usually mid to late July). Under cloudy conditions, cloud covered areas are later removed from the analysis.

2. Tape to Disk Data Transfer: Task TI. If CCT is obtained from the Prince Albert Satellite Receiving Station (PASS), or from another installation with identical AVHRR tape format, the CCT may be read to disk using format file AMHTF0001 which resides on backup tape # SRC780. There are five channels to be read from tape; the number of output data lines per channel is 2048. See Annex A for format file parameters.

3. Sub-Area Creation: Task AP. Display the entire image you have read to disk (channel 2 is recommended since it provides greatest image contrast, which facilitates geographic orientation) and create a sub-area of the area of interest. Be generous in your selection of boundaries so as not to eliminate study area margins.

4. Image Rotation (if necessary): Tasks AR & RS. Images which were acquired on the satellite's ascending pass will be inverted on the CRT display. Task AR allows the preparation of a polynomial transform file which, when applied to the data using task RS, rotates the image by 180. Resampling should be done using the nearest neighbour option.

5. Geometric Correction: Tasks GI & RS. Perform image to image registration. The slave image is the image under analysis, while the master image is N85FF8502, which resides on tape SRC832. The standard error estimate in the line and pixel directions should be less than nominal image resolution (approximately 1000 metres) for a satisfactory correction. Best results are accomplished using channel 2 of the slave image.

6. Haze Correction: Tasks PD & NO. Channels 1 and 2 must be adjusted for the additive effects of atmospheric scattering. Using task PD, determine the DN obtained for large, turbidity-free lakes. Subtract this value (as a negative offset) from channels 1 and 2 using task NO.

7. Calculate NDVI: Task NO. Calculate the normalized difference vegetation index using the "difference over sum" option of task NO. In order to be compatible with previous analysis, enter 145 and 31 when prompted for gain and offset, respectively.

Note: the preceding methodology provides an NDVI image compatible with those discussed in Part 2 of this Report. In order to evaluate this image with respect to the influence of precipitation during the growing season, proceed with the following steps:

8. Display Crop District Boundaries: Task ID. Crop District Boundaries may be overlaid by displaying theme file N85TTCMAP which resides on tape SRC755.

9. Extract NDVI Statistics for Crop Districts: Tasks IT & TS. Create training areas using Crop District Boundaries as guidelines using task IT. Lakes and cloud covered areas should be excluded. Extract average NDVIs for each training area (crop district) using task TS.

10. Obtain Precipitation Statistics. From the Environment Canada publication "Climatic Perspectives - Monthly Summary", obtain precipitation statistics for the primary climate observing stations noted in Figure 1.

11. Prepare Precipitation Distribution Map The data obtained in the preceding step may be summarized by plotting isohyets using a plotting software package. The isohyet maps shown in Figures 2 of this Report were plotted using the "SURFACE II" package. The program used for this plotting is shown in Annex C of this Report.

12. Extract Precipitation Statistics for Crop Districts. Crop District Boundaries may now be overlaid or transferred to the precipitation distribution map by using a "Map-O-Graph" or "Zoom Transfer Scope". Thus the average precipitation for each crop district may be estimated and compared using regression techniques to the NDVI data to determine the strength of the influence of precipitation on vegetation vigour.

FOR PART 3 (Forest Fire Detection)

1. Data Acquisition. Acquire NOAA AVHRR data having Local Area Coverage (LAC) (with spatial resolution at nadir of 1.1 km). These data should have geographic coverage of the area of interest, with the area of interest near the centre of the image swath so that pixels are of a minimum size. Care should be taken to ensure a minimum of cloud cover (if area of interest is not cloud-free, subsequent analysis is not possible). Data should be a 5-channel CCT.

2. Tape to Disk Data Transfer: Task TI. If CCT is obtained from the Prince Albert Satellite Receiving Station (PASS), or from another installation with identical AVHRR tape format, the CCT may be read to disk using format file AMHTF0001 which resides on backup tape # SRC780. There are five channels to be read from tape; the number of output data lines per channel is 2048. See Annex A for format file parameters.

3. Sub-area Creation: Task AP. Display the entire image you have read to disk (channel 2 is recommended since it provides greatest image contrast, which facilitates geographic orientation) and create a sub-area of the area of interest. Be generous in your selection of boundaries so as not to eliminate study area margins.

4. Histogram Acquisition: Task SH. For AVHRR channel 3, acquire the image's histogram and display it using the full data range possible (ie. 0-255). Examine the histogram, searching for pixels which have saturated at the bottom end (ie. DN 0) or are separate from the normal distribution of data, near DN 0. If any such pixels exist, proceed. If not, you may cease analysis, since no fires are detectable on the image. Fires which may exist might not be detected due to obstruction by clouds, low temperature in relation to actual pixel size, small fire size in relation to actual pixel size, or some combination of these factors. For an example histogram, see Annex B.

5. Image Rotation (if necessary): Tasks AR & RS. Images which were acquired on the satellite's ascending pass will be inverted on the CRT display. Task AR allows the preparation of a polynomial transform file which, when applied to the data using task RS, rotates the image by 180. Resampling should be done using the nearest neighbour option.

6. Geometric Correction: Tasks GI and RS. Perform image to image registration. The slave image is the image under analysis, while the master image is NGCFFCHN2, which resides on tape SRC781. The standard error estimate in the line and pixel directions should be less than nominal image resolution (approximately 1000 meters) for a satisfactory correction. Best results are accomplished using channel 2 of the slave image.

7. Image Density Slicing: Task CA. Channel 3 may now be density sliced. Theme 1's bounds should be DN 0-1, while theme 2's should be DN 2-9, or as indicated by the data as shown in histogram (step 4).

8. Grid Generation: Task GG. Generation of a UTM grid for overlay provides geographic reference so that the position of detected fires may be determined. A 50 pixel (50 km) grid provides sufficient detail without obscuring too many pixels.

ANNEX A

Parameters For Reading NOAA AVHRR Data Tape Produced at PASS ASCII Parameter File AMHTF0001:

```
IMAGE PARAMETER FILE = AMHTF0001.TFF;1


 TAPES IN DATASET   1
 ------------------------------------------------------------------------
 VOLSER          TAPE SEQUENCE NUMBER   1
 ------------------------------------------------------------------------
 ASCII HEADER RECORDS N  NUMBER OF RECORDS   0
 ------------------------------------------------------------------------
 ------------------------------------------------------------------------
 DATAFILES Y  NUMBER     1  SCANLINES     9999  PIX/LINE    2048
 ------------------------------------------------------------------
------
 FNUM  CHNS  FILSKP  RECSKP  FREC/L  RECSIZ  PDTH  BSF  ANF  PERD  NOGP
    1     5      2       1       5    2700     1    N    N     0     0
 ------------------------------------------------------------------------
    PHYSICAL RECORD NUMBER   1  NUMBER OF CHANNELS IN RECORD   1
       CHANNEL NO   NAME   PERIOD/LINE   DATAOS   CHANNEL TYPE
                1   CHN1              1      248          FF
    PHYSICAL RECORD NUMBER   2  NUMBER OF CHANNELS IN RECORD   1
       CHANNEL NO   NAME   PERIOD/LINE   DATAOS   CHANNEL TYPE
                1   CHN2              1      248          FF
    PHYSICAL RECORD NUMBER   3  NUMBER OF CHANNELS IN RECORD   1
       CHANNEL NO   NAME   PERIOD/LINE   DATAOS   CHANNEL TYPE
                1   CHN3              1      248          FF
    PHYSICAL RECORD NUMBER   4  NUMBER OF CHANNELS IN RECORD   1
       CHANNEL NO   NAME   PERIOD/LINE   DATAOS   CHANNEL TYPE
                1   CHN4              1      248          FF
    PHYSICAL RECORD NUMBER   5  NUMBER OF CHANNELS IN RECORD   1
       CHANNEL NO   NAME   PERIOD/LINE   DATAOS   CHANNEL TYPE
                1   CHN5              1      248          FF
```

ANNEX B

Example Histogram

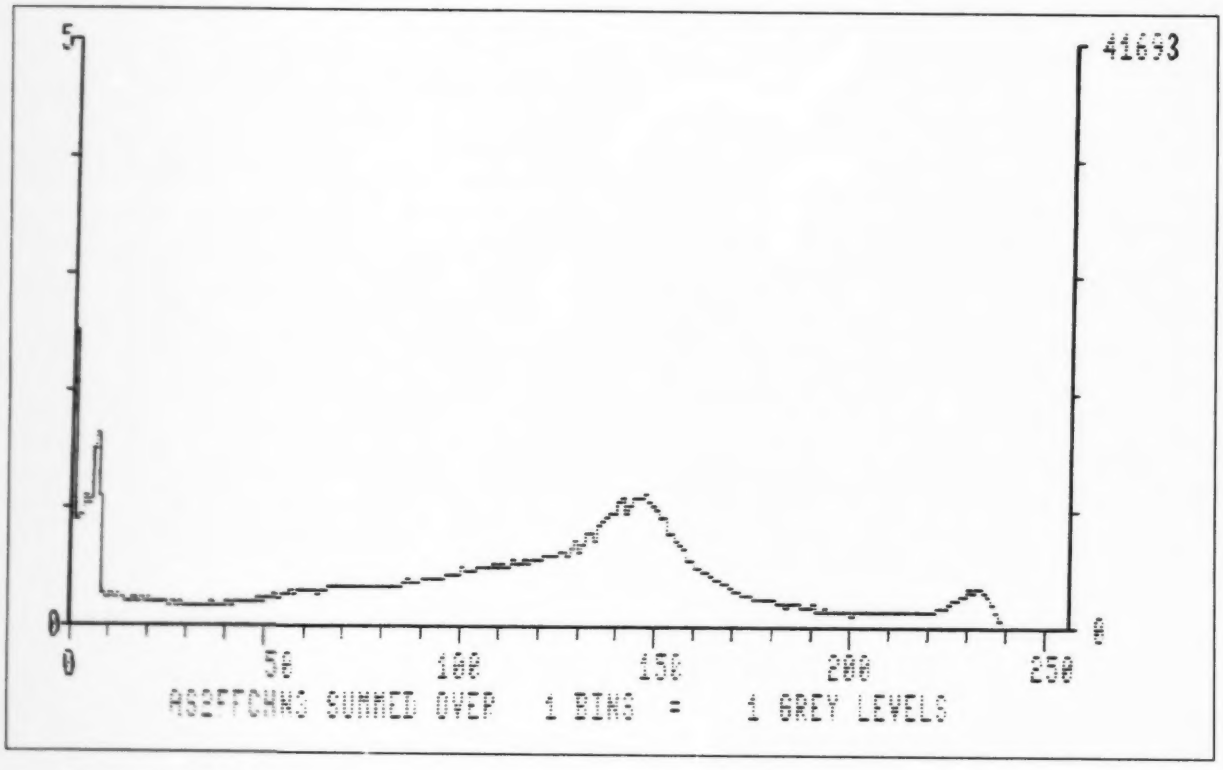

Histogram of July 3, 1985 Image

ANNEX C

Surface II Program for Creating Isohyet Map (of the kind shown in Figures 2 of this Report)

File precip.surface2

```
DEVI 1,'HOUGHAM',14,14,,,
IDXY 25,20,3,1,2,3,,,1,99.9,'(F4.1,1X,F4.1,16X,F4.1)'
ECHO
GRID 0,35,35,1,1,0,0
EXTR 0,27,0,25
CONT 1,1,,1,,,,
CINT 0,10,5,0,1,0.15,0,,0
SIZC 1,7,8
POST 2,,,,2
ROUT 22,1,'(2F4.1)'
ECHO
POUT
TITL  SASK. AVERAGE MONTHLY PRECIPITATION (MM) TO IMAGE DATE
PERF
STOP
```

File for022.dat
(outline data file)

```
  18    0
 4.546.2
 1.8 1.3
 6.0 1.2
 8.0 1.1
12.0 1.0
18.0 1.1
21.0 1.3
24.0 1.5
25.7 1.6
25.0 6.7
24.014.0
23.022.0
22.029.4
20.746.2
16.046.0
13.045.9
 8.046.0
 4.546.2
```

File for020.dat
(sample data file)

```
 2.3 23.9 60.8 55.3 43.6 68.1
 3.4 43.3 40.2 45.9 25.5 57.0
22.5  7.0 57.3 38.1 36.8 60.1
17.7 38.6 99.9 50.7 56.7 99.9
11.0 35.3 51.9 44.4 50.5 62.8
21.2  1.8 28.1 37.3 30.7 73.2
21.8 17.5 99.9 61.9 59.0 49.2
 5.0 11.8 36.5 41.6 31.6 45.6
14.4 26.3 68.7 55.1 54.4 77.6
 6.9 22.4 54.9 60.3 46.1 79.9
14.2  6.8 64.7 17.3 35.3 43.4
18.0 19.6 77.3 57.4 79.4 99.9
 7.1 16.9 64.3 51.4 51.8 68.7
13.4 18.5 55.6 65.4 57.8 54.7
16.7  7.2 98.6 24.9 38.6 62.3
11.2 14.1 74.9 32.7 51.6 58.6
 8.1  6.5 61.4 31.8 21.2 61.9
 7.3 44.3 99.9 44.7 28.2 99.9
17.5 12.7 99.8 43.0 53.0 49.2
22.2 10.7 99.9 53.0 49.9 68.1
23.7 33.5 61.1 34.8 60.5 73.1
24.5 21.4 93.9 53.2 46.6 58.2
```